Impact of Software-Defined Radio Transmitter on the Efficiency of RF Wireless Power Transfer

Nachiket Ayir
Unit of Electrical Engineering
Tampere University
Tampere, Finland
nachiket.ayir@tuni.fi

Taneli Riihonen
Unit of Electrical Engineering
Tampere University
Tampere, Finland
taneli.riihonen@tuni.fi

***Abstract*—In this paper, we experimentally examine the impact of a digital radio transmitter on radio-frequency (RF) wireless power transfer (WPT). The test-bed for this purpose consists of a software-defined radio (SDR) transmitter, an external power amplifier (PA), a variable attenuator to emulate the high losses in wireless propagation, and an RF energy harvesting receiver. The test-bed facilitates determining the transmitter efficiency and overall DC–DC efficiency of different test waveforms for RF WPT. We assess the performance of multisine signals as well as an information-bearing quadrature phase-shift keying (QPSK) signal for RF WPT, under different channel conditions, by determining the transmitter, DC–DC and receiver efficiency. The experiments reveal that high peak-to-average power ratio constraints the maximum RF output power for multisine signals. Even with similar input average power, single sinusoid RF waveforms yield the highest DC–DC and receiver efficiency. Moreover, a QPSK signal with transmit filtering provides good efficiency for WPT and seems to be a waveform suitable for simultaneous wireless information and power transfer applications.**

***Index Terms*—Wireless power transfer (WPT), RF energy harvesting, software-defined radio (SDR), non-linear distortion.**

I. Introduction

The concept of Internet of Things envisions an online network of millions of sensors, many of which would be deployed in places with no access to power plugs or replacing batteries. Far-field radio-frequency (RF) wireless power transfer (WPT) has the potential to suffice the demand of a replenishable energy source. This can be accredited to the drop in the energy consumption of sensors for their operational tasks.

A majority of the theoretical research in RF WPT has been on topics such as rectenna (a portmanteau for the combination of a receiver antenna and an RF diode-based rectifier) modeling, transmitter and receiver beamforming algorithms as well as waveform design and optimization. Moreover, the paradigm of simultaneous wireless information and power transfer (SWIPT) is being studied in terms of resource allocation at the transmitter, and time or power splitting techniques at the receiver. An exhaustive summary of such research works has been presented in [1]. On the practical research front, researchers have developed test-beds to study the impact of factors such as antenna directivity, beamforming, multiple energy sources, multiple antennas, on the total harvested energy. A brief survey of test-beds is available in [2].

This research was partially supported by the Ulla Tuominen foundation and the Academy of Finland under the grants 310991/326448 and 315858.

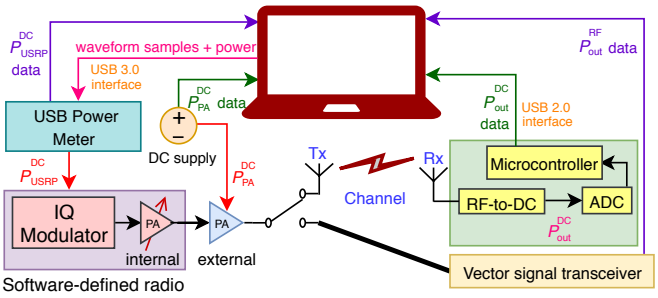

Fig. 1. Block diagram of the RF WPT test-bed.

The diode-based receiver has been extensively studied in RF WPT literature. Both theoretical [1] and experiment-driven [3] models have been developed to maximize the receiver efficiency. Many of the studies focusing on optimizing the rectifier efficiency have led to the conclusion that multisine waveforms exhibiting high peak-to-average power ratio (PAPR) are suitable for RF WPT [1], [4]. However, the impact of transmitter characteristics on the efficiency of RF WPT is yet to be explored in depth. The authors in [1], [5] conclude that the role of a transmitter in the overall RF WPT/SWIPT system performance needs to be studied practically.

In this paper, we investigate the transmitter-side performance in terms of the bandwidth analysis and DC–RF efficiency of different test waveforms, and later study its impact on the overall DC–DC efficiency of RF WPT. Specifically, we test the performance of multisine signals for WPT and an information-bearing quadrature phase-shift keying (QPSK) signal for SWIPT. Our earlier research work [2] evaluated the DC–DC efficiency of multisine signals for RF power transfer over a fixed wired channel without considering the impact of transmitter efficiency and high-power amplification.

II. System Model

In order to assess the performance of baseband waveforms for RF WPT, we developed a software-defined radio (SDR) test-bed which was first reported in [2]. In the latest revision, we have incorporated an external power amplifier (PA) and a

variable attenuator into the test-bed. A vector signal transceiver (VST) is also included to evaluate the transmitter efficiency. A block diagram of the improved test-bed is presented in Fig. 1, while its picture is shown in Fig. 2. The test-bed enables us to measure the overall DC–DC efficiency ($\eta_{\text{DC-DC}}$), as well as the transmitter-side DC–RF efficiency ($\eta_{\text{DC-RF}}$) for any waveform.

The transmitter side comprises a computer, a USB power meter, an SDR and an external PA. The computer generates the digital baseband waveforms and transfers them to the SDR. Moreover, the computer also supplies DC power to the SDR ($P^{\text{DC}}_{\text{USRP}}$), which is measured by the USB power meter and reported back to the computer. In order to facilitate wireless transmission, an external PA is employed to amplify the SDR's output RF signal and transmit it over the channel. A DC bench supply powers the external PA and reports power consumption data ($P^{\text{DC}}_{\text{PA}}$) to the computer. Thus, the total DC power supplied at the transmitter side is $P^{\text{DC}}_{\text{in}} = P^{\text{DC}}_{\text{USRP}} + P^{\text{DC}}_{\text{PA}}$.

In order to avoid any high-power co-channel interference into the used spectrum, we have used a wired channel. To be able to simulate the different attenuation levels of a flat-fading wireless channel, we have incorporated a programmable variable attenuator in the channel. The attenuation levels of the channel are set by the computer. The other option would be to perform the experiments in an anechoic chamber. While measuring the power of the transmitted RF signal ($P^{\text{RF}}_{\text{out}}$) with the VST, we utilize a wired channel as well.

The receiver side constitutes a VST while measuring $P^{\text{RF}}_{\text{out}}$, and an RF energy harvesting receiver while measuring $P^{\text{DC}}_{\text{out}}$. In the former case, the VST reports $P^{\text{RF}}_{\text{out}}$ to the computer where $\eta_{\text{DC-RF}}$ is computed. In the latter case, the RF energy harvester that is equipped with a diode-based rectifier converts the incident RF power ($P^{\text{RF}}_{\text{in}}$) to DC power. The energy harvester board is accompanied by an analog-to-digital converter (ADC) and a microcontroller to continuously sample the rectified DC power across an onboard resistor R and report the same to the computer. The computer first calculates the average harvested DC power ($P^{\text{DC}}_{\text{out}}$) and then the corresponding $\eta_{\text{DC-DC}}$, which for a RF WPT system is defined as

$$\eta_{\text{DC-DC}} = \frac{P^{\text{DC}}_{\text{out}}}{P^{\text{DC}}_{\text{in}}} = \left(\frac{P^{\text{RF}}_{\text{out}}}{P^{\text{DC}}_{\text{in}}}\right) \times \left(\frac{P^{\text{RF}}_{\text{in}}}{P^{\text{RF}}_{\text{out}}}\right) \times \left(\frac{P^{\text{DC}}_{\text{out}}}{P^{\text{RF}}_{\text{in}}}\right) = \eta_{\text{DC-RF}} \times \eta_{\text{RF-RF}} \times \eta_{\text{RF-DC}}, \quad (1)$$

where $\eta_{\text{RF-RF}}$ and $\eta_{\text{RF-DC}}$ represent the channel efficiency and receiver efficiency, respectively. The SDR used in this research work is a Universal Software Radio Peripheral (USRP).

A co-phased N-tone multisine signal used in the experiments is given by

$$x(t) = A \sum_{n=1}^{N} \exp\left(j\, 2\pi n f_0\, t + j\, \frac{\pi}{4}\right), \quad (2)$$

where A denotes the amplitude of the multisine signal, while f_0 represents the fundamental frequency. The phase value $\frac{\pi}{4}$ ensures that the signals on the in-phase (I) and quadrature-phase (Q) branches of the USRP are similar (i.e., mirror images of each other). The analysis of USRP [2] reveals that the digital-to-analog converter (DAC) in the USRP has an input range of ± 1 for discrete baseband samples, and complex input samples' magnitude should not exceed one.

The waveforms in the I and Q branches merge after up-conversion to RF producing an N-tone multisine-modulated RF waveform with power $\alpha N A^2/2$, where α represents the internal scaling factor of the USRP. The RF waveform is then amplified by the internal PA of the USRP and transmitted. Thus, by setting $A = \frac{c}{N}$, $c \leq 1$, we get an undistorted multisine-modulated RF waveform at the output of USRP.

Since amplification by USRP's internal PA is insufficient for wireless power transmission, an external PA is required. The internal PA of the USRP has a variable gain of G_{USRP} [dB], while the external PA has a fixed gain of G_{PA} [dB] in the linear amplification region (LAR). The output power of the

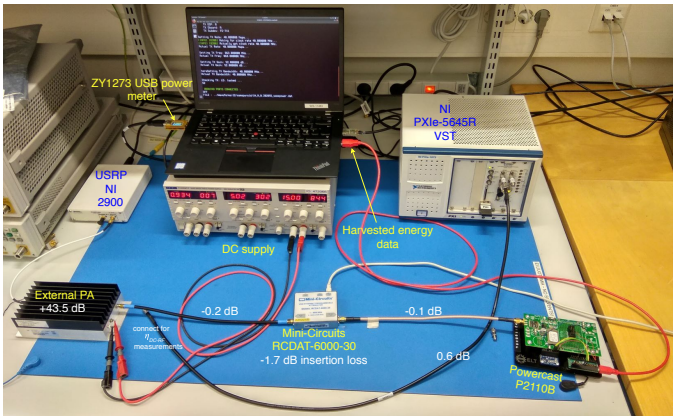

Fig. 2. RF WPT test-bed for measuring $\eta_{\text{DC-DC}}$ and $\eta_{\text{DC-RF}}$.

TABLE I
HARDWARE CONFIGURATION FOR THE TEST-BED.

Component	**Product details**
Computer	Lenovo ThinkPad T470p, 32GB RAM, Core i7 processor, Linux OS, GNU C++ compiler
SDR	National Instruments USRP-2900
USB power meter	YZXStudio ZY1273
External PA	Mini-Circuits ZHL-4240+
Variable attenuator	Mini-Circuits RCDAT-6000-30
RF energy harvester	Powercast P2110B
VST	National Instruments PXIe-5645R

TABLE II
OPERATIONAL PARAMETERS FOR THE EXPERIMENTS.

Parameter	**Details**
Frequency band	863–873 MHz (unlicensed)
Carrier frequency	$f_{\text{c}} = \begin{cases} 863 \text{ MHz}, & \text{multisine} \\ 868 \text{ MHz}, & \text{QPSK} \end{cases}$
Sampling rate	40 MHz
Baseband fundamental frequency	$f_0 = 1$ MHz
Number of tones in multisine	$N \in [1, 10]$
USRP gain setting	$G_{\text{USRP}} \in [45, 69.5]$ dB (with 0.5 dB steps)
R	286 Ω
c	0.6
β	-78 dB

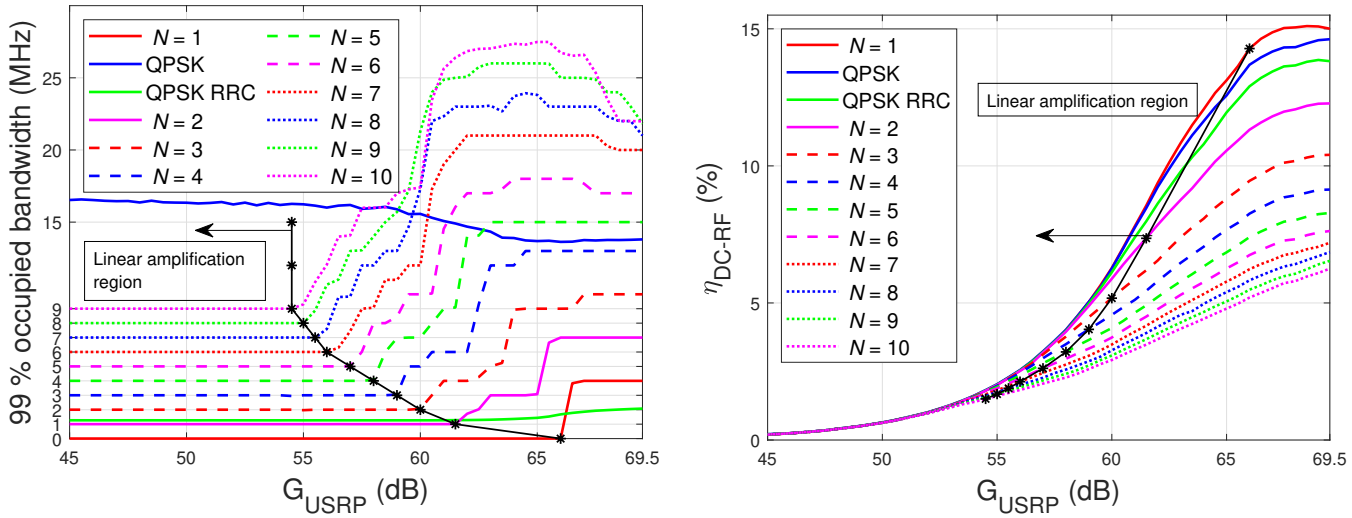

(a) Bandwidth occupied by 99% of $P_{\text{out}}^{\text{RF}}$ at varying G_{USRP}

(b) Transmitter efficiency for varying G_{USRP}

Fig. 3. Measured spectral response of the multisines and QPSK waveforms to determine the linear amplification region and the corresponding $\eta_{\text{DC-RF}}$.

external PA ($P_{\text{out}}^{\text{RF}}$) can be represented (in logarithmic scale) as

$$\begin{aligned} P_{\text{out}}^{\text{RF}} &= G_{\text{PA}} + G_{\text{USRP}} + 10\log_{10}(\alpha N A^2/2) \\ &= \beta + G_{\text{USRP}} + 20\log_{10} A + 10\ \log_{10} N \\ &= \beta + G_{\text{USRP}} + 20\log_{10} c - 10\ \log_{10} N, \end{aligned} \tag{3}$$

where $\beta = G_{\text{PA}} + 10\log_{10}(\alpha/2)$ is a constant to be determined experimentally. It must be noted that $P_{\text{out}}^{\text{RF}}$ is independent of $P_{\text{in}}^{\text{DC}}$ in the LAR. In fact, $P_{\text{USRP}}^{\text{DC}}$ and $P_{\text{PA}}^{\text{DC}}$ only determine the bias point of their respective power amplifiers in the LAR. Now, using (3), we can determine the value of $P_{\text{out}}^{\text{RF}}$ for an N-tone multisine signal, for a given c and G_{USRP}. In order to observe the performance of multisines in RF WPT, it is essential to operate in the LAR of both the PAs, which leads to lower $P_{\text{out}}^{\text{RF}}$ as we shall see in the next section.

III. Experimental Setup and Results

The hardware configuration of the test-bed is presented in Table I, and the operational parameters for the experiments are shown in Table II. Along with multisines varying from $N = 1$ to 10, we have also considered two forms of 1 Msps QPSK[1] waveforms ($\pm 0.707 \pm 0.707j$): one without any transmit filter and one with a root raised cosine (RRC) transmit filter (with roll-off of 0.5). This helps us to study the viability of SWIPT in terms of both $\eta_{\text{DC-DC}}$ and bandwidth. Each transmission was about five seconds long and the results presented here have been averaged over five such transmissions.

A few important observations regarding $P_{\text{out}}^{\text{RF}}$ are as follows:

- The maximum $P_{\text{out}}^{\text{RF}}$ for a given N, without any significant non-linear distortion, can be achieved by many different combinations of G_{USRP} and c.
- The permissible input RF power rating of the external PA (occurs at $G_{\text{USRP}} = 69.5$ dB in our experiments) and G_{PA} are the factors limiting the maximum $P_{\text{out}}^{\text{RF}}$.

[1]We choose a QPSK baseband signal since the corresponding RF signal is simply a sinusoidal signal with phase transitions at symbol rate. This allows for a fair comparison with the $N = 1$ case.

In order to have a fair comparison, we chose the amplitude values such that all the waveforms have similar $P_{\text{out}}^{\text{RF}}$. This also allows us to ascertain the impact of PAPR of a multisine waveform on WPT. For example, multisines with $N = 3$ and 4 will have similar $P_{\text{out}}^{\text{RF}}$, but PAPR of 6 and 8, respectively.

First, we try to figure out the LAR for multisine waveforms. To do so, we vary G_{USRP} and measure the bandwidth occupied by signal containing 99% of $P_{\text{out}}^{\text{RF}}$. The VST samples the RF signal and the analysis is performed in MATLAB. The results are shown in Fig. 3a. In the LAR, 99% bandwidth of an N-tone multisine with $f_0 = 1$ MHz is about $(N-1)f_0$, while that of an RRC filtered 1 Msps QPSK signal is around 1.27 MHz. We observe in Fig. 3a that the LAR goes on reducing as N increases, which is expected since higher PAPR leads to non-linear distortion at lower G_{USRP}. We also observe how the RRC filter drastically reduces the bandwidth of QPSK signal, and confines within the channel bandwidth. Notice that for $G_{\text{USRP}} < 54$ dB, the multisine waveforms operate in the LAR.

The importance of linear operation can be seen in Fig. 3b, where we present the $\eta_{\text{DC-RF}}$ of waveforms for varying G_{USRP}. As expected, for $G_{\text{USRP}} < 54$ dB, all the waveforms have similar $\eta_{\text{DC-RF}}$ since they all operate in the LAR and have the same $P_{\text{out}}^{\text{RF}}$. As non-linear distortion takes over, $P_{\text{out}}^{\text{RF}}$ and hence $\eta_{\text{DC-RF}}$ increase slowly with increasing G_{USRP}. A simple sinusoid at RF ($N = 1$) has the lowest PAPR, *viz.* two, and hence has the largest LAR. Consequently, across the whole range of G_{USRP}, it has the highest $\eta_{\text{DC-RF}}$ while $N = 10$ yields the lowest $\eta_{\text{DC-RF}}$. The WPT efficiency of QPSK is similar to $N = 1$ case for $G_{\text{USRP}} \leq 62.5$ dB, while it is a bit lower at higher gains due to the non-linearity introduced by the sharp transitions between symbols. Although RRC filtering reduces them for QPSK, the corresponding RF waveform is no longer a simple sinusoid, which explains the reduction in $\eta_{\text{DC-RF}}$, as it suffers from non-linear distortion at lower G_{USRP} compared to $N = 1$ and standard QPSK. However, the RRC-filtered waveform still yields better efficiency than the multisines.

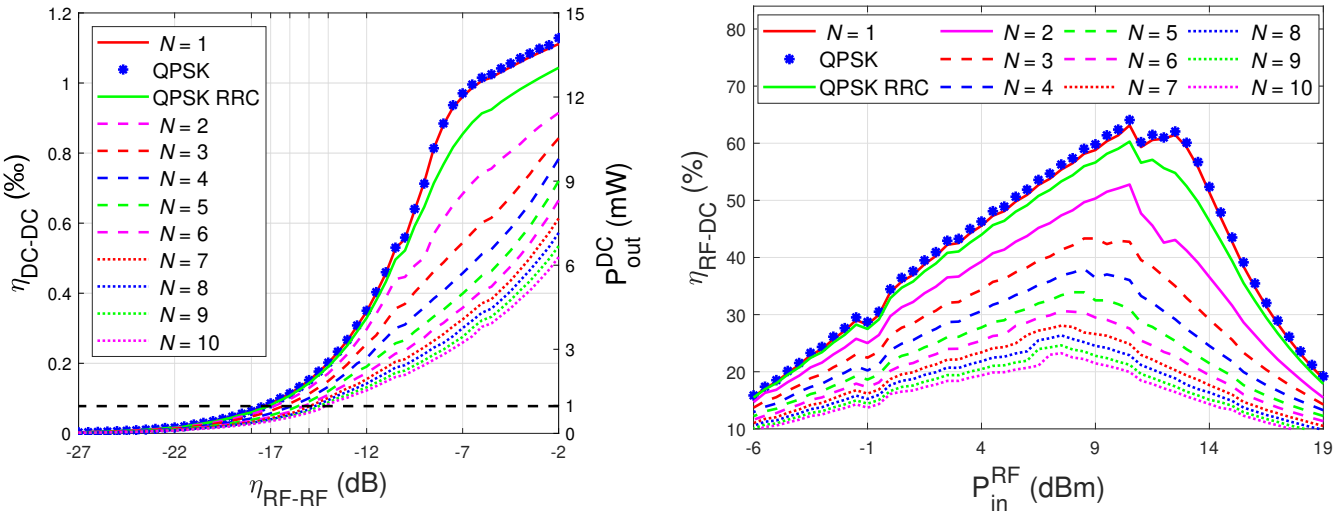

(a) Overall DC–DC efficiency of waveforms for $P_{\text{out}}^{\text{RF}} \approx 21$ dBm

(b) Receiver efficiency of waveforms at different input power levels

Fig. 4. Measured $\eta_{\text{DC-DC}}$ of RF WPT in terms of the $\eta_{\text{RF-RF}}$ and the $\eta_{\text{RF-DC}}$ computed from it versus the $P_{\text{in}}^{\text{RF}}$.

Based on the observations of Fig. 3, we have, henceforth, set $G_{\text{USRP}} = 52$ dB, which gives $P_{\text{out}}^{\text{RF}} \approx 21$ dBm. Now, we vary $\eta_{\text{RF-RF}}$ by varying the channel attenuation and compute the overall DC–DC efficiency ($\eta_{\text{DC-DC}}$). An important parameter in WPT is the amount of $P_{\text{out}}^{\text{DC}}$ harvested at different $\eta_{\text{RF-RF}}$ levels, since this will eventually decide the practical range of RF WPT. Both these results are shown in Fig. 4a. $\eta_{\text{DC-DC}}$ is presented in permil levels. We observe that the single sinusoid waveforms ($N = 1$ and QPSK) outperform all the other waveforms at high and moderate $\eta_{\text{RF-RF}}$ (low and moderate channel attenuation) levels. However, as the channel attenuation increases above 20 dB ($\eta_{\text{RF-RF}} \leq -20$ dB), all the waveforms tend to have very low $\eta_{\text{DC-DC}}$. Another observation is that to obtain reasonable $P_{\text{out}}^{\text{DC}} \approx 1$ mW, $P_{\text{in}}^{\text{RF}}$ needs to be about $21 - 18 = 3$ dBm for $N = 1$, while as high as about $21 - 14 = 7$ dBm for $N = 10$, which is more than twice the $P_{\text{in}}^{\text{RF}}$ for a single sinusoid case.

Finally, $\eta_{\text{RF-DC}}$ was computed using (1) and the results are shown in Fig. 4b. Again, the single sinusoid RF waveforms have the highest $\eta_{\text{RF-DC}}$ of about 64% at $P_{\text{in}}^{\text{RF}} \approx 11$ dBm followed by RRC filtered QPSK and $\eta_{\text{RF-DC}}$ keeps decreasing as N increases. The minor jaggedness observable in Fig. 4b possibly occurs due to fluctuations in the operating conditions of the components during the experiments. Overall, Figs. 3b, 4a, and 4b reveal that apart from the high attenuation losses in wireless medium, the significant other reason for low $\eta_{\text{DC-DC}}$ in RF WPT is the low $\eta_{\text{DC-RF}}$ at the transmitter.

IV. Conclusion and Future Work

An RF WPT test-bed system for evaluating the transmitter efficiency and overall DC–DC efficiency was presented. It was experimentally observed that the amplitude of multisine signals needs to be scaled down heavily to avoid severe non-linear distortion caused due to the USRP's internal PA. The spectral analysis helped us to identify the region of linear amplification for the waveforms in terms of the USRP gains. Higher the multisine's PAPR, lower was the maximum operable USRP gain for linear amplification, and thus worse was the transmission efficiency at higher gains. For a fair comparison of the overall DC–DC efficiency between various waveforms, we chose the USRP gain such that all the waveforms were linearly amplified and thus had the same output RF power. The channel attenuation was varied to simulate a wireless scenario. We observed again that higher the number of multisines, lower was both the DC–DC efficiency and the receiver efficiency.

In the case of information-bearing signals, the RRC-filtered QPSK waveform fares better than all the multisine signals, except for the single sinusoid, in all the parameters. Moreover, it complies with bandwidth requirements and, thus, appears to be a waveform appropriate for real-world SWIPT applications. In future work, we analyze the WPT performance of different modulations. Moreover, the impact of varying parameters such as the bit-rate, frequency band, transmitter–receiver distance, reflectors, will be examined in an actual wireless setup.

References

[1] B. Clerckx, R. Zhang, R. Schober, D. W. K. Ng, D. I. Kim, and H. V. Poor, "Fundamentals of wireless information and power transfer: From RF energy harvester models to signal and system designs," *IEEE Journal on Selected Areas in Communications*, vol. 37, no. 1, pp. 4–33, Jan. 2019.

[2] N. Ayir, M. F. Trujillo Fierro, T. Riihonen, and M. Allén, "Experimenting waveforms and efficiency in RF power transfer," in *Proc. IEEE MTT-S International Microwave Symposium (IMS)*, Jun. 2019, pp. 1140–1143.

[3] E. Boshkovska, D. W. K. Ng, N. Zlatanov, and R. Schober, "Practical non-linear energy harvesting model and resource allocation for SWIPT systems," *IEEE Communications Letters*, vol. 19, no. 12, pp. 2082–2085, Dec. 2015.

[4] A. Boaventura, D. Belo, R. Fernandes, A. Collado, A. Georgiadis, and N. B. Carvalho, "Boosting the efficiency: Unconventional waveform design for efficient wireless power transfer," *IEEE Microwave Magazine*, vol. 16, no. 3, pp. 87–96, Apr. 2015.

[5] S. Claessens, N. Pan, M. Rajabi, D. Schreurs, and S. Pollin, "Analysis of modulation techniques for SWIPT with software defined radios," in *Proc. 37th WIC Symposium on Information Theory*, May. 2016, pp. 9–16.